Effect of Gas Phase Chemical Reactions on Heat Transfer to a Charring Ablator

A. F. MILLS*
University of California, Los Angeles, Calif.

AND

A. V. GOMEZ†
TRW Systems Group, Houston, Texas

AND

G. STROUHAL‡
NASA Manned Spacecraft Center, Houston, Texas

Numerical solutions have been obtained for multicomponent stagnation-point flow with mass transfer of ablation products yielded by the phenolic-novalac Apollo command module heat shield. Equilibrium chemistry is assumed, and the range of pertinent parameters such as stagnation enthalpy and pressure, and pyrolysis gas and char elemental compositions, are typical of re-entry from a lunar mission. The results for the various components of the surface energy flux may be used for the evaluation of heat shield performance during Apollo re-entry. Corresponding to each exact solution, inert injectant heat and mass transfer correlations were used to estimate the surface heat transfer q_u on the assumption that all the ablation product reactions take place at the ablator surface. The ratio $q_u(\text{exact})/q_u(\text{inert}) \equiv \mathcal{R}$, termed the chemical energy recovery factor, is near unity for most cases of practical significance. The factor $\mathcal{R}$ essentially isolates the effects on surface heat transfer of gas-phase chemical reactions involving the ablation products. Furthermore, using our results, we are able to demonstrate an ablation prediction procedure which should prove suitable for many engineering purposes.

Nomenclature

a = species weighting constant
B = injection rate parameter, $\dot{m}/g^*$
C_p = specific heat at constant pressure
D = reference diffusion coefficient
$\mathfrak{D}$ = binary diffusion coefficient
F = diffusion factor
g = conductance
H,h = total and static enthalpies
j = diffusive mass flux
k = thermal conductivity
K = number of chemical elements
Le = Lewis number $\rho C_p \mathfrak{D}/k$
M = molecular weight
m = mass fraction
$\dot{m}$ = mass transfer rate
n = absolute mass flux or number of chemical species
p = pressure
q = conductive heat flux
R_N = nose radius
r = radius from axis of symmetry
$\dot{r}$ = species production by chemical reaction
$\mathcal{R}$ = chemical energy recovery factor, q_u (exact numerical solution)/q_u (inert injectant solution)
s,y = coordinates along and normal to surface
T = temperature
u,v = velocity components parallel and normal to surface
x = mole fraction
δ = boundary-layer thickness
ρ = density
μ = dynamic viscosity
ϕ = fraction of steady-state value of $\dot{m}_c/\dot{m}_g$

Subscripts

c,g = char and pyrolysis gas, respectively
e = edge of boundary layer
es = mixture of edge gas composition but at the surface temperature
h,m = heat and mass transfer, respectively
i,j = chemical species i, j
mono = monatomic molecule of identical molecular weight
o = stagnation point
s,u = s surface and u surface
t = transferred state
(α) = chemical element (α)

Superscripts

B,MC = binary and multicomponent, respectively
$*$ = zero mass transfer
(t) = total diffusive

Introduction

THE most refined method of predicting heat transfer to a charring ablator presently available involves the coupling of a numerical solution procedure for the boundary-layer flow conservation equations to a finite-difference solution procedure for the in-depth response of the ablative material.[1] Such an approach is not feasible for performing engineering calculations over a complete re-entry trajectory because of the cost and the inherent unreliability of such a complex computer program. Thus, current practice involves a finite-difference solution of the conservation equations governing the

---

Presented as Paper 70-869 at the AIAA 5th Thermophysics Conference, Los Angeles, Calif., June 29–July 1, 1970; submitted December 29, 1970; revision received February 8, 1971. This study was conducted for NASA/MSC in support of E&DD Task E-45B.

[*] Assistant Professor of Engineering and Applied Science. Member AIAA.

[†] Staff Engineer, Aeromechanics Laboratory. Member AIAA.

[‡] Aerospace Engineer, Thermal Technology, Structures and Mechanics Division. Member AIAA.

in-depth response of the ablator but uses simple correlation formulas to describe the convective heat transfer to the ablator surface. These formulas are in the form of standard correlations for high-temperature boundary-layer flows with correction factors to account for the reduction of heat transfer due to surface mass addition. The most extensive computations of these "blockage" factors are those of Anfimov[2] and Gomez et al.,[3] but are restricted by the assumption that the injected gases do not react within the boundary layer. The objective of this study was to compute the data required to evaluate the effect on the surface heat transfer of gas-phase chemical reactions involving the ablation products. The specific ablator considered is that used for the heat shield of the Apollo command module, i.e., a fiber-glass phenolic matrix containing an epoxy-novalac resin with phenolic microballoons and silica-fiber reinforcement; the aerothermochemical environment studied is typical of re-entry from a lunar mission. In addition, the data presented allow us to demonstrate a heat-transfer prediction procedure suitable for engineering calculations. A computer program based on this procedure is currently in production use at NASA/MSC for the evaluation of the Apollo heat shield performance.

The basic data were generated by obtaining numerical solutions for axisymmetric stagnation-point flow with surface mass addition. Multicomponent diffusion and a general equilibrium chemical environment are considered. Unequal diffusion coefficients are accounted for, with sufficient accuracy, through use of Kendall's bifurcation approximation for the binary diffusion coefficients. Thermal diffusion and diffusional conduction are assumed to have a negligible effect on the heat transfer. Absorption and emission of thermal radiation are ignored. The ranges of pertinent parameters considered are characteristic of re-entry from a lunar mission. The results presented here, in particular the various components of the surface energy flux, have direct engineering application. Of equal concern however is the development of an appropriate correlation procedure.

Most analyses of chemically reacting boundary-layer flows have been performed utilizing the simplifying assumption of unity effective Lewis numbers for all diffusing species. Numerous correlation procedures[4-7] have been proposed in order to account for the effect of nonunity Lewis numbers on the surface heat transfer. Paucity of suitable data has precluded a comprehensive evaluation of the merits of the various procedures and, as a result, no single procedure is presently accepted as being satisfactory. Bartlett, Nicolet, and Howe[8] correlated a heat-transfer conductance defined as the surface diffusive energy flux $k\partial T/\partial y|_s + \Sigma j_{i,s}h_{i,s}$ divided by the enthalpy difference $(H_e - h_s)$; the corresponding correlation of the enthalpy h_s is, of course, also required. An alternative procedure would be to provide separate correlations of the conduction component in the form $k\partial T/\partial y|_s$ divided by $(H_e - h_{es})$ and the species diffusive fluxes $j_{i,s}$ in the form of mass transfer conductances $g_{m,i}$. A correlation of h_s is again required to complete the surface energy balance. However, the mass transfer conductances are themselves of direct interest for various purposes.

In this work we have chosen to use yet another approach to the correlation of data for the surface heat transfer. Our rationale is as follows: ablation has essentially two effects on the boundary-layer flow, 1) a reduction of the surface heat conduction and species diffusive fluxes due to blowing, in a manner similar to that for inert foreign gas injection, and 2) heat release or absorption due to chemical reactions; e.g., there is the possibility of exothermic combustion involving the edge gases, or endothermic dissociation of product species such as CO_2 and H_2. In the present application the dominant gas-phase ablation product reactions are usually the endothermic dissociations. For $Le = 1$ there is the well-known result[4,9] that the surface heat transfer is independent of the location of dissociation reactions within the boundary layer; i.e., they may be assumed to occur at the surface. Thus, we suggest that the effect of ablation on heat transfer may be viewed as primarily due to blowing, with an injectant gas composition consistent with the assumptions that all the ablation product reactions take place at the surface. The additional effect of the precise location of the reactions within the boundary layer is then expected to be relatively minor and hence conveniently correlated for engineering purposes.

To isolate the effect of gas-phase chemical reactions the following procedure is followed. For boundary conditions identical to those of a particular exact numerical solution, inert injectant heat and mass transfer correlations[3] are used in a calculation of the surface heat transfer, in which it is assumed that all the chemical reactions take place at the surface. The required injectant composition ($m_{i,ts}$; $i = 1,2,\ldots,n$) is obtained by performing an open system equilibrium chemical state computation in which both the reactions of the pyrolysis gases and char surface with the freestream air are included. As an end result the ratio q_u (exact numerical solution)/q_u (inert injectant solution) = $\mathcal{R}$, termed the chemical energy recovery factor, is calculated. This parameter is a measure of the effect of gas-phase reactions on the surface heat transfer, but of course also reflects errors inherent in the empirical content of the inert injectant calculations.

Finally, this $\mathcal{R}$ factor suggests the basis for an engineering ablation prediction procedure. One can include an open-system, surface chemical state computation at each time step of the finite-difference solution for the in-depth response of the ablator. Thus, the heat transfer to the ablator surface is calculated on the assumption that all the ablation product reactions take place at the surface, i.e., in a manner identical to that just described for q_u (inert injectant solution). Previously generated correlations of $\mathcal{R}$ for the specific ablator under consideration may then be incorporated to correct the inert injectant solution. Since $\mathcal{R}$ usually is quite near unity, the procedure has merit for general engineering purposes. A situation for which the procedure might not be appropriate is, for example, towards the end of re-entry where the heat shield could essentially burn, with a dominance of exothermic gas phase reactions.

Analysis

Numerical Solutions

A coordinate system is chosen such that distances measured along and normal to the surface are s and y respectively; the corresponding velocity components are u and v. For steady axisymmetric stagnation point boundary-layer flow, the governing conservation equations for a nonradiating, multicomponent, chemically reacting gas mixture are

mass:

$$(\partial/\partial s)(\rho ur) + (\partial/\partial y)(\rho vr) = 0 \tag{1}$$

momentum:

$$\rho u\, \partial u/\partial s + \rho v\, \partial u/\partial y = \rho_e u_e\, du_e/ds + (\partial/\partial y)(\mu\, \partial u/\partial y) \tag{2}$$

species:

$$\rho u \frac{\partial m_i}{\partial s} + \rho v \frac{\partial m_i}{\partial y} = \frac{\partial}{\partial y}(-j_i) + \dot{r}_i \quad i = 1,2,\ldots,n \tag{3}$$

total enthalpy:

$$\rho u \frac{\partial H}{\partial s} + \rho v \frac{\partial H}{\partial y} = \frac{\partial}{\partial y}\left(k\frac{\partial T}{\partial y} - \sum_i j_i h_i\right) + \frac{\partial}{\partial y}\left(u\mu\frac{\partial u}{\partial y}\right) \tag{4}$$

The Shvab-Zeldovich transformation is applied to the species conservation equations to yield conservation equations for

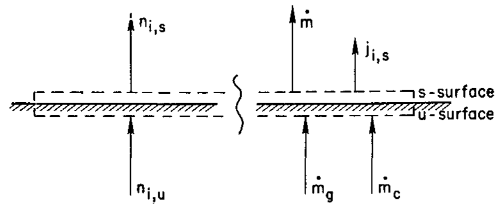

Fig. 1 Surface mass fluxes.

the chemical elements:

$$\rho u \frac{\partial m_{(\alpha)}}{\partial s} + \rho v \frac{\partial m_{(\alpha)}}{\partial y} = \frac{\partial}{\partial y}[-j_{(\alpha)}]; \quad (\alpha) = 1,2,\ldots,K \quad (5)$$

where

$$m_{(\alpha)} = \sum_{i=1}^{n} m_{(\alpha),i} m_i; \quad j_{(\alpha)} = \sum_{i=1}^{n} m_{(\alpha),i}\, j_i$$

The diffusion fluxes j_i are obtained from the Chapman-Enskog kinetic theory of gases.[9] To uncouple the Stefan-Maxwell equations describing these fluxes, a bifurcation approximation[10-12] to the binary diffusion coefficients is introduced in the form

$$\mathcal{D}_{ij} = \bar{D}(T,p)/F_i F_j \quad (6)$$

where $\bar{D}(T,p)$ is a reference binary diffusion coefficient and $F_i(T)$ is a property of the ith species, called a diffusion factor. For the present investigation it was adequate to take the F_i independent of temperature and employ the simple correlation of the form recommended by Kendall,[12] namely

$$F_i \propto M_i^{0.461} \quad (7)$$

With these simplifications the diffusion flux j_i becomes

$$j_i = -(\rho \bar{D} \mu_2/\mu_1 M)[\partial z_i/\partial y + (z_i - m_i)\partial \ln \mu_2/\partial y] \quad (8)$$

where

$$z_i = M_i x_i/F_i \mu_2; \quad \mu_1 = \sum_j x_j F_j$$

$$\mu_2 = \sum_j M_j x_j/F_j; \quad M = \sum_j x_j M_j$$

The stagnation-point velocity gradient $[du_e/ds]_0$ is obtained in the conventional manner by combining the Euler equation applied at the outer edge of the boundary layer with the Newtonian pressure distribution for stagnation point flow to yield

$$(du_e/ds)|_0 = (1/R_N)(2p_{e,0}/\rho_{e,0})^{1/2} \quad (9)$$

where R_N is taken as 10 ft, a value appropriate for the Apollo command module. The boundary conditions appropriate to the problem are

$$y \to \infty: \quad u \to u_e(s); \quad m_{(\alpha)} \to m_{(\alpha),e}; \quad H \to H_0 \quad (10)$$

$$y = 0: \quad u = 0 \quad (11)$$

$$\dot{m} = \dot{m}_g + \dot{m}_c = \rho_s v_s \quad (12)$$

$$m_{(\alpha),t}\, \dot{m} = m_{(\alpha),s} \dot{m} + \sum_{i=1}^{n} m_{(\alpha),i} j_{i,s}; \quad (\alpha) = 1,2,\ldots,K \quad (13)$$

where the boundary condition given by Eq. (13) has been cast in the form suggested by Spalding.[13] Figure 1 illustrates the notation.

The viscosities and thermal conductivities of the pure components, and $\bar{D}$ are computed in the manner recommended by Hirschfelder, Curtiss, and Bird.[9] The Lennard-Jones interaction potential is assumed, and the required parameters are obtained from Svehla[14] and Hochstim.[15] The mixture viscosity is calculated following the method of Wilke,[16] and the mixture thermal conductivity according to Mason and Saxena.[17] The diffusion factors F_i are computed from Eq. (7); in addition, solutions have been obtained using more accurate values of F_i appropriate to the chemical system under consideration. The results obtained by the two methods show no significant differences. Thermodynamic properties from the JANAF tables[18] and Duff-Bauer[19] are used.

A NASA/MSC computer program, originally developed by the Aerotherm Corporation, is used. The numerical procedure[20] is based on the method of weighted residuals with square-wave moment functions and spline interpolation functions for the primary dependent variables. Kendall[20] demonstrated that three place accuracy could generally be obtained with seven spline segments. The resultant set of algebraic relations is solved by Newton-Raphson iteration using matrix inversion. The chemical state and required state derivatives were computed in a standard manner.[21] Computer time for a set of 7 solutions is typically 5 min on a Univac 1108 machine.

Chemical Energy Recovery Factor $\mathcal{R}$

For each exact numerical solution a corresponding inert injectant solution was obtained as follows. For identical values of $\dot{m}_g, m_{(\alpha),g}, m_{(\alpha),c}, T_s$ and external flow parameters, an open system surface equilibrium chemical state computation[21] was made. The required elemental constraints are provided by the set of elemental flux relations

$$m_{(\alpha),t}\dot{m} = m_{(\alpha),s}\dot{m} + \sum_{i=1}^{n} m_{(\alpha),i} j_{i,s}; \quad (\alpha) = 1,2,\ldots,K \quad (14)$$

where

$$j_{i,s} = g_{m,i}(m_{i,s} - m_{i,e}) \quad (15)$$

The mass transfer conductances $g_{m,i}$, and a suitable expression for the surface conductive heat flux q_s, were obtained from the inert injectant multicomponent mass and heat transfer correlations developed by Gomez et al.,[3] namely

$$g_{m,i}{}^{MC}/g_{m,i}{}^{*} = a_m{}^{MC} B_h/[\exp(a_m{}^{MC} B_h) - 1]; \quad B_h = \dot{m}/g_h{}^{*} \quad (16)$$

where

$$a_m{}^{MC} = 1.125\left(M_{\text{air}} \sum_{i=1}^{n} \frac{m_{i,ts}}{M_i}\right)^{2/3}; \quad m_{i,ts} = \frac{n_{i,s}}{\dot{m}} \quad (17)$$

$$q_s{}^{MC}/q_s{}^{*} = \prod_{i=1}^{n}\left[\frac{q_s{}^{B}(B_{h,i})}{q_s{}^{*}}\right] \quad (18)$$

where

$$q_s{}^{B}/q_s{}^{*} = a_{h,i} B_{h,i}/[\exp(a_{h,i} B_{h,i}) - 1] \quad (19)$$

$$a_{h,i} = 1.25\left(\frac{M_{\text{air}}}{M_i}\right)_s^{0.4}\left(\frac{C_{pi}}{C_{pi,\text{mono}}}\right)_s^{0.3}; \quad B_{h,i} = \frac{n_{i,s}}{g_h{}^{*}} \quad (20)$$

The exponential functional forms are suggested by Couette flow modeling of the boundary layer. The multicomponent combining rules, Eqs. (17) and (18), and the species weighting constants a_i are empirical. The product form of Eq. (18)

Table 1 Pyrolysis gas and char elemental mass fractions

	Chemical model I, no coking		Model II, 100% coking	
Element	$m_{(\alpha),g}$	$m_{(\alpha),c}$	$m_{(\alpha),g}$	$m_{(\alpha),c}$
Hydrogen	0.093	0	0.131	0
Carbon	0.547	0.511	0.361	0.614
Nitrogen	0.019	0	0.027	0
Oxygen	0.341	0.238	0.481	0.206
Silicon	0	0.251	0	0.180

was first suggested by Anfimov.[2] Consistent with the manner in which the mass transfer conductance correlations were developed, the composition $m_{i,e}$ in Eq. (15) was taken to be that of a gas mixture of freestream elemental composition in equilibrium at the surface temperature.

This chemical state computation yields the char removal rate $\dot{m}_c$, the molecular composition at the s surface $m_{i,s}$, and the transferred state mass fractions $m_{i,ts}$. These values of $m_{i,ts}$ are essential to the calculation of q_s since in Eq. (20) there appears $n_{i,s} = m_{i,ts}\dot{m}$. A surface energy balance may now be constructed to yield the conductive heat flux into the ablator q_u

$$q_u = k(\partial T/\partial y)|_s + \left[\sum_i n_{i,s}h_{i,s} - \sum_i n_{i,u}h_{i,u}\right] \quad (21)$$

Finally, $\mathcal{R}$ is calculated:

$$\mathcal{R} = q_u(\text{exact numerical solution})/ q_u(\text{inert injectant solution}) \quad (22)$$

Results

Two chemical models were postulated to describe the characteristics of phenolic-novalac ablation under Apollo re-entry conditions:

1) The pyrolysis gases do not react with the char as they percolate to the surface.

2) The pyrolysis gases are in chemical equilibrium with the char at the surface temperature. In particular "coking" reactions have occurred resulting in a deposition of carbon in the char. Table 1 gives the elemental mass fractions appropriate to the two models.

Steady-state ablation is defined as the situation where the char surface and the pyrolysis zone recede at identical rates. For chemical models I and II, the steady-state values of $\dot{m}_c/\dot{m}_g$ are 0.898 and 1.699, respectively. Computations were performed for $\phi = 0.1$, 0.5, and 1.0 [ϕ = (actual $\dot{m}_c/\dot{m}_g$)/(steady-state value)]. The low values of ϕ characterize the ablator behavior early in the re-entry trajectory. Table 2 presents results of the exact numerical solutions, which allow a surface energy balance to be constructed in the form given by Eq. (23). Also presented are values of $q_s^{(t)} = k\partial T/\partial y|_s + \Sigma_i j_{i,s}h_{i,s}$ and h_s from the inert injectant calculations, together with the resulting values of $\mathcal{R}$. The parameters are ϕ, H_e, p, and B_h. The enthalpies are with respect to enthalpy datum states consistent with the JANAF tables.[18] Figure 3 illustrates species concentration profiles through the boundary layer.

Discussion

The Numerical Solutions

Presented in Table 2 are the surface heat transfer q_u, and the zero mass addition surface heat transfer q^*. The values of q_u, or preferably q_u/q^* may be graphed or correlated to provide engineering data. In evaluating the accuracy of such data, three sources of error may be identified: 1) the numerical solution procedure itself (as discussed already, the three-place accuracy asserted is a negligible source of error in the present context); 2) the data used to compute the thermodynamic and transport properties (complex gas mixtures at 4000–23,000°R are involved, and the transport properties, which are essentially theoretical predictions without direct experimental confirmation, must be particularly suspect); and 3) the bifurcation approximation to the $\mathcal{D}_{ij}$ (this error is probably no larger than the expected error in the $\mathcal{D}_{ij}$ diffusion coefficients themselves[11]). With the inadequacy of the high-temperature transport property data particularly in mind, an error in q_u/q^* of between 5 and 10% is suggested.

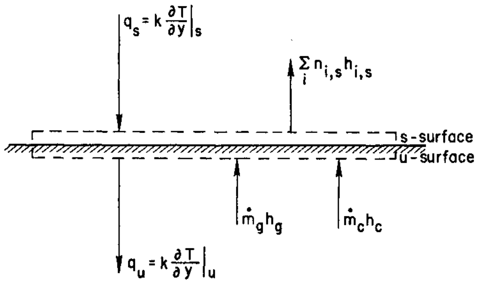

Fig. 2a Surface energy balance: absolute basis.

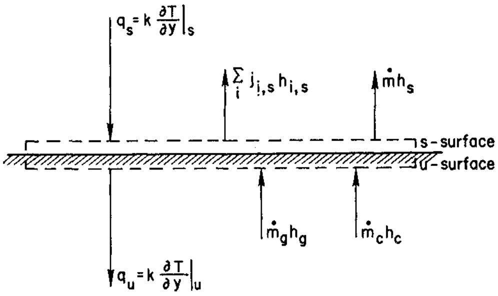

Fig. 2b Surface energy balance: convective and diffusive components.

Heat-Transfer Correlation Procedures

Numerous procedures have been proposed for the correlation of heat transfer from chemically reacting boundary-layer flows. An understanding of the essential features of any given procedure with regard to ablation calculations requires a careful study of the surface energy balance. Figures 2a and 2b illustrate the surface energy balance written in two different forms: 1) with the species fluxes in absolute terms, and 2) with the species fluxes separated into convective and diffusive components. To avoid unnecessary algebraic complexity, absorption and emission of radiation, and mechanical removal of surface material are not included in the energy balances which follow. The data and procedures of the present study are independent of these effects; their inclusion simply requires use of the appropriate form of the surface

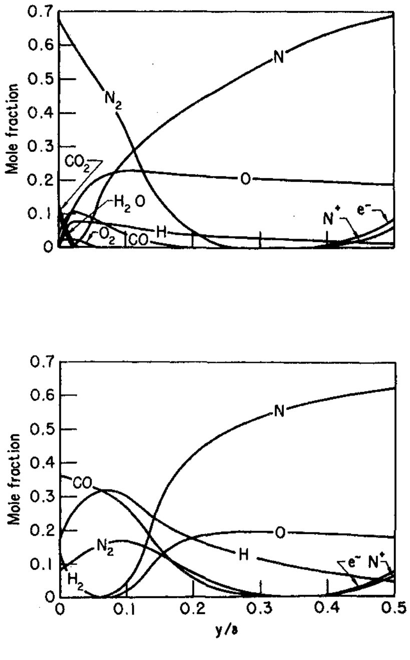

Fig. 3 Concentration profiles, Cases No. 1-I and 29-I

Table 2 Exact numerical solutions, inert injectant calculations, and the chemical energy recovery factor ℛ

				Chemical Model I												Chemical Model II											
No.	ϕ	H_e	p	B_h	T_s	h_s		q^*	$q_s^{(t)}$		$\dot{m}h_s$	$\dot{m}_g h_g$	$\dot{m}_c h_c$	q_u	$\mathcal{R}$	B_h	T_s	h_s		q^*	$q_s^{(t)}$		$\dot{m}h_s$	$\dot{m}_g h_g$	$\dot{m}_c h_c$	q_u	$\mathcal{R}$
						exact	inert		exact	inert								exact	inert		exact	inert					
		$\frac{Btu}{lb}$	atm		°R	$\frac{Btu}{lb}$	$\frac{Btu}{lb}$	$\frac{Btu}{ft^2\text{-}s}$	$\frac{Btu}{ft^2\text{-}s}$	$\frac{Btu}{ft^2\text{-}s}$	$\frac{Btu}{ft^2\text{-}s}$	$\frac{Btu}{ft^2\text{-}s}$	$\frac{Btu}{ft^2\text{-}s}$	$\frac{Btu}{ft^2\text{-}s}$			°R	$\frac{Btu}{lb}$	$\frac{Btu}{lb}$	$\frac{Btu}{ft^2\text{-}s}$	$\frac{Btu}{ft^2\text{-}s}$	$\frac{Btu}{ft^2\text{-}s}$	$\frac{Btu}{ft^2\text{-}s}$	$\frac{Btu}{ft^2\text{-}s}$	$\frac{Btu}{ft^2\text{-}s}$	$\frac{Btu}{ft^2\text{-}s}$	
1	.10	25000	1.00	.109	4537	49	71	312.3	313.4	285.2	.1	2.3	- .4	315.2	1.098	.109	4600	179	210	312.1	311.5	282.9	.3	2.2	- .4	313.0	1.101
2	"	"	"	.544	5449	1882	1769	306.3	200.0	192.8	13.4	23.4	- 1.6	208.3	1.032	.544	4041	174	95	314.7	228.0	212.7	1.2	7.0	- 2.4	231.3	1.068
3	"	"	"	1.091	5949	4727	4730	300.3	98.4	103.7	67.5	83.5	- 3.0	111.2	.957	1.087	5018	1907	1905	309.8	120.6	105.5	27.2	31.7	- 3.7	121.2	1.144
4	"	"	"	1.638	5987	6070	6004	299.7	56.8	50.5	130.0	129.3	- 4.4	51.4	1.118	1.630	5369	3396	3375	307.0	60.0	50.6	72.7	67.3	- 5.0	49.2	1.237
5	.10	25000	1.00	1.091	5949	4727	4730	300.2	98.4	103.7	67.5	83.5	- 3.0	111.2	.957	1.087	5018	1907	1905	309.8	120.6	105.5	27.2	31.7	- 3.7	121.2	1.144
6	"	20000	"	1.107	5935	4693	4703	231.7	81.1	79.0	67.0	82.0	- 3.0	93.0	1.029	1.100	5018	1961	1904	241.0	107.6	81.8	28.0	31.8	- 3.7	107.4	1.306
7	"	15000	"	1.099	5928	4809	4591	168.3	70.5	59.0	68.7	81.3	- 3.0	80.0	1.122	1.081	5013	1978	1868	179.3	81.8	63.6	28.2	31.6	- 3.7	81.2	1.262
8	"	10000	"	1.062	5920	4807	4421	106.9	42.8	40.9	68.6	80.4	- 3.0	51.5	.940	1.048	5021	2028	1799	116.9	58.6	45.1	29.0	31.8	- 3.7	57.5	1.219
9	.10	25000	.05	1.325	5568	6793	6987	65.7	10.6	17.0	26.0	29.2	- .9	12.8	.699	1.307	4960	3584	3608	68.5	16.6	17.7	13.7	14.2	- 1.0	15.9	.942
10	"	"	.10	1.430	5652	6654	6784	93.5	14.8	21.0	39.1	41.9	- 1.3	16.3	.757	1.416	5062	3620	3634	96.9	21.3	21.6	21.2	21.0	- 1.5	19.5	.999
11	"	"	.50	1.322	5872	5617	5685	211.1	48.1	54.6	68.5	76.5	- 2.6	53.3	.908	1.314	5197	2917	2888	217.8	64.0	55.6	35.6	36.3	- 3.0	61.5	1.159
12	"	"	1.00	1.091	5949	4727	4730	300.2	98.4	103.7	67.5	83.5	- 3.0	111.2	.957	1.087	5018	1907	1905	309.8	120.6	105.5	27.2	31.7	- 3.7	121.2	1.144
13	"	"	5.00	1.322	6237	5006	5017	673.5	187.3	171.5	194.2	216.1	- 7.6	201.2	1.092	1.318	5475	2657	2605	689.2	227.2	173.8	103.1	104.1	- 8.8	219.0	1.312
14	.50	25000	1.00	.109	4770	298	309	311.1	306.7	285.8	.4	1.8	- 1.4	306.6	1.073	.109	4792	349	369	311.1	306.9	285.1	.5	1.4	- 1.3	306.5	1.077
15	"	"	"	.544	5539	1985	1768	305.3	203.4	193.1	14.2	17.5	- 6.1	200.3	1.046	.543	4974	1210	1079	310.2	219.9	194.6	8.6	8.5	- 6.0	213.4	1.130
16	"	"	"	1.093	6046	4637	4589	299.0	102.3	106.6	66.2	61.2	-11.0	85.7	.956	1.090	5853	3949	3906	301.5	110.3	106.8	56.4	40.2	- 9.0	84.8	1.051
17	"	"	"	1.640	6079	5741	5745	297.1	49.5	54.1	123.0	93.8	-16.4	3.1	.541	1.637	5915	5020	5067	300.7	52.2	53.7	107.5	64.4	-13.1	- 4.7	.706
18	.50	25000	1.00	1.093	6046	4637	4589	299.0	102.3	106.6	66.2	61.2	-11.0	85.7	.956	1.090	5853	3949	3906	301.5	110.3	106.8	56.4	40.2	- 9.0	84.8	1.051
19	"	20000	"	1.108	6026	5563	4559	230.2	82.0	81.1	65.2	59.7	-11.1	65.0	1.029	1.106	5833	3882	3851	232.9	89.4	81.8	55.4	39.3	- 9.0	63.8	1.154
20	"	15000	"	1.100	6006	4514	4453	167.2	63.0	60.3	64.5	58.3	-11.1	45.2	1.067	1.096	5815	3834	3752	170.0	67.3	61.4	54.7	38.5	- 9.1	41.5	1.167
21	"	10000	"	1.064	6000	4600	4285	105.6	44.8	41.4	65.7	57.9	-11.1	25.3	.994	1.059	5807	3921	3595	108.5	53.6	42.7	56.0	38.1	- 9.1	26.2	1.393
22	.50	25000	.05	1.328	5669	6328	6461	64.1	11.2	18.0	24.2	20.6	- 3.2	4.3	.419	1.323	5511	5638	5763	66.0	12.7	18.0	21.6	14.4	- 2.7	2.7	.378
23	"	"	.10	1.434	5749	6238	6342	92.9	14.8	184.2	36.6	29.9	- 4.8	3.0	.319	1.428	5592	5523	5633	93.9	16.6	22.3	32.4	20.7	- 4.0	.7	.140
24	"	"	.50	1.322	5967	5394	5422	210.1	48.5	59.0	65.8	55.4	- 9.6	28.0	.786	1.321	5795	4684	4742	212.1	52.2	57.2	57.1	37.9	- 7.8	24.7	.893
25	"	"	1.00	1.093	6046	4637	4589	299.0	102.3	106.6	66.2	61.2	-11.0	85.7	.956	1.090	5853	3949	3906	301.5	110.3	106.8	56.4	40.2	- 9.0	84.8	1.051
26	"	"	5.00	1.324	6334	484[illegible]	4856	671.0	185.9	179.1	187.9	157.9	-28.1	126.4	1.088	1.322	6145	4173	4218	675.5	195.9	178.8	161.9	105.6	-21.6	116.9	1.240
27	1.00	25000	1.00	.109	4845	416	410	311.0	301.7	286.5	.6	1.3	- 2.1	300.2	1.053	.109	4844	415	407	311.0	301.6	286.3	.6	.9	- 1.7	300.2	1.054
28	"	"	"	.544	5661	2112	1911	304.1	203.0	193.5	15.1	13.8	- 9.1	174.9	1.042	.544	5677	2134	1956	304.0	202.7	192.9	15.2	9.8	- 6.6	190.4	1.050
29	"	"	"	1.094	6131	4529	4451	297.5	107.7	108.4	64.5	45.1	-16.5	56.2	1.010	1.094	6138	4543	4482	297.4	107.5	107.4	64.9	31.8	-10.9	63.0	1.020
30	"	"	"	1.642	6173	5992	5538	296.8	47.8	56.8	128.3	-24.5	-36.8	1.231	1.755	1.642	6179	5564	5583	296.8	47.7	55.9	119.2	48.9	-16.1	-39.4	1.113
31	1.00	25000	1.00	1.094	6131	4529	4451	297.5	107.7	108.4	64.5	45.1	-16.5	56.2	1.010	1.094	6138	4543	4482	297.4	107.5	107.4	64.9	31.8	-10.9	63.0	1.020
32	"	20000	"	1.110	6118	4496	4453	229.0	84.2	82.4	64.2	44.5	-16.5	47.1	1.061	1.110	6125	4511	4466	228.9	84.1	81.7	64.4	31.4	-11.0	39.5	1.104
33	"	15000	"	1.102	6093	4404	4353	166.0	61.0	103.1	62.9	43.2	-16.6	23.9	1.031	1.102	6100	4418	4353	165.9	60.9	60.6	63.1	30.5	-11.1	16.6	1.082
34	"	10000	"	1.067	6075	4397	4176	104.5	43.6	41.4	62.8	42.4	-16.7	5.6	1.082	1.067	6082	4410	4169	104.4	45.3	41.1	63.0	29.9	-11.2	.5	-.249
35	1.00	25000	.05	1.332	5763	5990	6020	64.7	12.6	18.6	22.9	14.9	- 4.8	- .5	-.113	1.332	5771	5998	6063	64.7	12.6	18.4	23.0	10.5	- 3.4	- 3.5	-2.62
36	"	"	.10	1.437	5848	5923	5989	91.1	15.6	23.2	34.8	21.7	- 7.2	- 5.1	-3.46	1.438	5855	5966	6029	91.1	15.5	22.9	35.0	15.3	- 5.0	- 9.5	2.637
37	"	"	.50	1.326	6065	5263	5228	209.9	50.2	59.0	64.2	40.9	-14.3	11.8	.604	1.326	6071	5276	5274	208.9	50.1	58.3	64.4	28.8	- 9.6	4.4	.418
38	"	"	1.00	1.094	6131	4529	4451	297.5	107.7	108.4	64.5	45.1	-16.5	56.2	1.010	1.094	6138	4543	4482	297.4	107.5	107.4	64.9	31.8	-10.9	63.0	1.020
39	"	"	5.00	1.325	6430	4778	4739	668.1	189.0	184.2	185.4	117.8	-41.9	77.4	1.109	1.325	6437	4795	4787	668.1	188.7	182.0	186.0	83.1	-25.8	58.6	1.264

energy balance. The two equations representing the energy balances depicted in Figs. 2a and 2b are, respectively

$$q_u = k(\partial T/\partial y)|_s - \sum_i n_{i,s}h_{i,s} + \dot{m}_g h_g + \dot{m}_c h_c \qquad (23)$$

$$q_u = k(\partial T/\partial y)|_s - \sum_i j_{i,s}h_{i,s} - \dot{m}h_s + \dot{m}_g h_g + \dot{m}_c h_c \qquad (24)$$

where Eq. (24) may be obtained from Eq. (23) by substituting the relations

$$n_{i,s} = \dot{m}m_{i,s} + j_{i,s}; \quad h_s = \sum_i m_{i,s}h_{i,s}$$

and q_u is the conductive heat flux into the heat shield. These equations are exact within the assumptions implied by the over-all problem statement. Most correlation procedures evolve from the form of Eq. (24) which obtains under the unity Lewis number assumption, namely

$$q_u = (k/C_p)(\partial h/\partial y)|_s - \dot{m}h_s + \dot{m}_g h_g + \dot{m}_c h_c \qquad (25)$$

If, in addition, the effect of viscous dissipation is simplified by assuming a unity Prandtl number (or alternatively if attention is restricted to stagnation point flow), and if the $\rho\mu$ product is constant across the boundary layer, then we have the exact result[4] that the appropriate driving force in a heat transfer correlation is the total enthalpy difference. Thus we write Eq. (25) as

$$q_u = g_h(H_e - h_s) - \dot{m}h_s + \dot{m}_g h_g + \dot{m}_c h_c \qquad (26)$$

where g_h is the heat-transfer conductance ($g_h \equiv \rho_e u_e St_h$ where St_h is the heat-transfer Stanton number). Comparison of Eqs. (24) and (26) shows that, in the general situation of $Le_i \neq 1$, this conductance must be defined as[8]

$$g_h \equiv \left[k(\partial T/\partial y)|_s - \sum_i j_{i,s}h_{i,s}\right]\Big/(H_e - h_s) \equiv q_s^{(t)}/(H_e - h_s) \qquad (27)$$

i.e., the conductance is based on the total energy flux relative to the mass average velocity $q_s^{(t)}$.

Table 3 Data from an inert injectant calculation with prescribed $\dot{m}_c$

	Chemical model I				Chemical model II			
Case No.	T_s, °R	h_s, Btu/lb	$q_s^{(t)}$, Btu/ft²-s	$\mathcal{R}$	T_s, °R	h_s, Btu/lb	$q_s^{(t)}$, Btu/ft²-s	$\mathcal{R}$
1	4542	74	285.3	1.098	4615	211	283.1	1.100
2	5627	2057	192.5	1.044	4040	144	194.4	1.169
3	5945	4709	104.2	0.948	4990	1838	106.7	1.119
4	4962	5929	51.0	1.058	5316	3226	51.5	1.107
5	5945	4709	104.2	0.948	4990	1838	106.7	1.119
6	5946	4726	79.6	1.022	4989	1834	82.8	1.272
7	5943	4627	59.5	1.117	4958	1755	64.4	1.212
8	5938	4468	41.1	0.943	4884	1581	45.9	1.122
9	5542	6867	17.2	0.673	4913	3377	18.0	0.876
10	5624	6685	21.2	0.727	5013	3421	22.0	0.916
11	5853	5622	55.0	0.886	5131	2698	56.4	1.088
12	5945	4709	104.2	0.948	4990	1838	106.7	1.119
13	6217	4970	172.7	1.070	5380	2431	176.5	1.236
14	4764	312	286.1	1.072	4792	371	285.6	1.075
15	5703	2102	194.3	1.052	5177	133	196.2	1.130
16	6035	4538	108.5	0.919	5840	3829	109.8	0.986
17	6053	5677	55.7	0.341	5888	4962	56.2	−3.392
18	6035	4538	108.5	0.919	5840	3829	109.8	0.986
19	6036	4564	82.8	0.989	5842	3854	84.1	1.084
20	6034	4515	51.6	1.033	5839	3809	63.1	1.101
21	6028	4349	42.1	0.965	5825	3622	43.8	1.260
22	5630	6320	18.4	0.379	5473	5585	18.7	0.310
23	5717	6232	22.9	0.283	5729	5487	23.2	0.117
24	5943	5346	58.7	0.724	5772	4627	59.2	0.765
25	6035	4538	108.5	0.919	5840	3829	109.8	0.986
26	6314	4802	183.1	1.010	6122	4118	185.1	1.080
27	4843	415	287.0	1.051	4843	415	287.0	1.051
28	5771	2116	195.4	1.040	5793	2159	195.3	1.042
29	6124	4401	111.3	1.140	6132	4423	111.3	0.920
30	6143	5468	59.2	2.743	6149	5483	59.3	1.524
31	6124	4401	111.3	1.140	6132	4423	111.3	0.920
32	6126	4442	84.7	0.974	6133	4457	84.7	0.967
33	6125	4411	62.8	0.936	6132	4425	62.8	0.906
34	6119	4274	42.4	0.918	6039	5149	61.0	0.283
35	5716	5880	19.3	−0.045	5722	5886	19.3	−0.878
36	5805	5865	24.1	−1.122	5811	5874	24.1	74.14
37	6033	5136	61.0	0.504	6039	5149	61.0	0.283
38	6124	4401	111.3	1.140	6132	4423	111.3	0.920
39	6409	4677	190.4	0.938	6416	4692	190.5	0.911

In order to provide the basis for alternative correlation procedures we now follow Lees[4] and rearrange Eq. (26) by subtracting and adding the term $\Sigma m_{i,e}h_{i,s}$ to obtain

$$q_u = g_h\left(H_e - \sum_i m_{i,e}h_{i,s}\right) + \sum_i g_h(m_{i,e} - m_{i,s})h_{i,s} - \dot{m}h_s + \dot{m}_g h_g + \dot{m}_c h_c \qquad (28)$$

Introducing the notation $h_{es} = \Sigma\, m_{i,e}h_{i,s}$, the enthalpy of a mixture of freestream composition but at the surface temperature, and noting that for $Le_i = 1$, $g_h = g_{m,i}$, Eq. (28) becomes

$$q_u = g_h(H_e - h_{es}) + \sum_i g_{m,i}(m_{i,e} - m_{i,s})h_{i,s} - \dot{m}h_s + \dot{m}_g h_g + \dot{m}_c h_c \qquad (29)$$

If we now define the mass transfer conductances as $g_{m,i} = j_{i,s}/(m_{i,e} - m_{i,s})$ even for $Le_i \neq 1$ and with gas phase reactions, then comparison of Eqs. (29) and (24) shows that

$$k(\partial T/\partial y)|_s = g_h(H_e - h_{es}) \qquad (30)$$

We now make two observations:

1) The separation of the conductive and interdiffusion contributions in Eq. (29) is exact even for a chemically reacting flow with $Le_i \neq 1$, provided that values of the conductances are obtained from an exact numerical solution. It is only when empiricism is introduced via the use of, for example, Reynolds analogy type correlations for the heat- and mass-transfer conductances, that the separation becomes inexact.

2) The energy flux across the s surface of direct concern is not the sum of the conduction and interdiffusion fluxes $q_s^{(t)}$ (termed the energy supplied by convection by Bartlett et al.[8]) but the conduction flux only. This is best seen from Eq. (23) which may be rewritten as

$$q_u = k(\partial T/\partial y)|_s + \left[\sum_i n_{i,s}h_{i,s} - \sum_i n_{i,u}h_{i,u}\right] \qquad (31)$$

The bracketed term is the energy absorbed or released *at the surface* due to chemical reaction or phase change. For example, for transpiration cooling with an inert gas, this term would be identically zero.

Thus, there is a definite merit to the idea of attempting to provide separate correlations for the conduction and diffusion components of $q_s^{(t)}$ in the form of the conductances g_h and $g_{m,i}$ defined by Eq. (29). Unfortunately the latter tend to behave anomalously when species are produced or consumed within the boundary layer; for a specific application an adequate correlation of the numerical data for $g_{m,i}$ proves complex and tedious. Since chemical equilibrium is assumed in the present application there is the alternative possibility of correlating elemental mass transfer conductances $g_{m,(\alpha)}$; but a loss in generality of the over-all procedure would be thereby incurred. In this light the decision of Bartlett et al.,[8] to correlate the total flux $q_s^{(t)}$ is understandable despite a number of objections which can be raised. Firstly, a separate correlation of h_s must still be provided in order to reconstruct the surface energy balance, Eq. (26). Secondly, the numerical value of $q_s^{(t)}$ is dependent on the chosen enthalpy datum state. Thus, engineering calculations based on such correlations must employ the identical datum state. Also, direct comparison cannot be made with energy fluxes that have absolute values such as q_s^* and radiative transfer.

The choice of a correlation procedure depends on the manner in which the correlations are intended for use. Thus, Bartlett et al.,[8] present detailed instructions for the use of their correlations in the engineering calculation of steady-state ablation, and they refer to a more general form of this engineering calculation intended for application to transient ablation. We have developed, and used extensively, a method for calculating the transient response of a charring ablator along a re-entry trajectory. The essential element of this method is the addition of an open system surface chemical state computation at all (or selected) time steps of a conventional finite difference solution for the in-depth response of the ablator. The solution proceeds as follows:

1) T_s, $\dot{m}_g$, and the $g_{m,i}$ are obtained from the previous time step; 2) with the known $m_{(\alpha)g,t}$ and $m_{(\alpha),e}$, an open system surface chemical state computation yields $\dot{m}_c$ and $m_{i,s}$; 3) the current value of q_s^* is calculated by a standard aerodynamic heating routine; 4) Eqs. (16–20) are used to obtain $m_{i,ts}$, q_s, and new values of $g_{m,i}$; 5) a surface energy balance is performed to yield q_u; and 6) with this value of q_u the finite-difference calculation of the in-depth response of the ablator yields new values of T_s and $\dot{m}_g$.

Addition of the surface chemistry computation to the calculation method provides a theoretical prediction of $\dot{m}_c$, a precise surface energy balance, and the values of $m_{i,ts}$ required to incorporate adequate heat and mass transfer correlations. The increase in computer time has proven to be less than 10% for the calculation of heat shield response along a re-entry trajectory.

The only significant assumption in the foregoing calculation method is that all the ablation product reactions take place at the surface of the ablator. The error incurred by making this assumption is negligible in many applications; thus the calculation method may be often used without further modification. The data obtained in the present study allow the method to be refined by introducing a correction for the effect of gas-phase reactions involving the ablation products. The conductive heat flux into the heat shield q_u determined in step 5 need be simply multiplied by $\mathcal{R}$ to recover the exact numerical solution. Also, as mentioned above, surface radiation and mechanical removal of surface material, may be accounted for by writing an appropriate form for the surface energy balance. The accuracy of the final result then depends only on the adequacy of correlations or tabulated data of $\mathcal{R}$ generated for the specific ablator. Since $\mathcal{R}$ usually is near unity, it is not difficult to insure that the corrected value of q_u is within a stipulated error limit.

In correlating our data in terms of $\mathcal{R}$ we are, therefore, both isolating the effect of gas-phase chemical reactions and providing a simple correction factor for use in an engineering calculation. Also, in basing our procedure on q_u, we are able to provide data which are independent of choice of enthalpy datum state. Of course $\mathcal{R}$ also corrects for errors introduced through the empirical inert injectant heat and mass transfer correlations; this is a desirable feature when used in an engineering calculation. On the other hand, this feature precludes an evaluation of the effects of gas phase chemical reactions in situations where $\mathcal{R} \approx 1$ or where q_u is relatively low.

An Alternative Definition of $\mathcal{R}$

The previous section stressed that our choice of correlation procedure was strongly influenced by the requirement that resulting data be in a form convenient for engineering calculations. In such a calculation $\dot{m}_g$ and T_s are determined by the finite-difference solution for the in-depth response of the ablator and may be prescribed for the surface state chemistry at the next time step. It was for this reason that inert injectant calculations corresponding to exact numerical solutions were obtained by matching values of $\dot{m}_g$ and T_s; the equilibrium surface chemical state computation then yielded the resulting values of $\dot{m}_c$. However, it is also possible to specify $\dot{m}_g$ and $\dot{m}_c$ in the chemical state computation; a T_s then results from the equilibrium chemistry requirement. Values of $\mathcal{R}$ calculated following this latter approach are presented in Table 3 for chemical models I and II respectively. These values of $\mathcal{R}$ are not too useful for engineering purposes but do throw additional light on the effects of gas-phase chemical reactions.

Trends Exhibited by $\mathcal{R}$

In discussing the trends exhibited by $\mathcal{R}$ in Table 2 it is convenient first to dispose of the anomalies which can be attributed to errors introduced by the inert injectant heat and mass transfer correlations, or by loss of accuracy in the over-all approach. We make the following observations:

1) At small B_h (Cases 1-I, 14-I, 27-I, 1-II, 14-II, 27-II) $1.05 \leq \mathcal{R} \leq 1.10$. Values much closer to unity would be expected owing to the relatively small quantity of ablation products being added to the boundary layer. It can be seen that for these cases $\mathcal{R}$ essentially mirrors the behavior of $q_s^{(t)}$. Also, comparison of the data in Tables 2 and 3 shows that matching $\dot{m}_c$ instead of T_s yields almost identical results. The anomaly results from a deficiency in the inert injectant heat transfer correlation at low injection rates when H and H_2 are present. For example, in Case 1-I the exact numerical value of $q_s^{(t)}$ is actually a little higher than q_s^*, even though $B_h = 0.109$. This is due to the increased mixture thermal conductivity, near the surface, which accompanies appreciable mole fractions of low molecular weight chemical species such as H and H_2. The exponential form of the inert injectant heat transfer correlation, Eq. (19), and the associated empirical constants were chosen to yield adequate predictions over a wide range of B_h and chemical species. It proved infeasible to substantially improve the correlation in this regime.

2) When $q_u \ll q_s^*$ or $\dot{m}h_s$, errors inherent in both the heat and mass transfer correlations are greatly magnified. The fact that q_u legitimately can become negative compounds the problem. Such situations occur when B_h is large and when H_e and p are small. Cases 35-II and 36-II are the most dramatic examples of this behavior. Again the data in Table 3 shows that whether T_s or $\dot{m}_c$ is matched with the exact solution has little effect on $q_s^{(t)}$. Fortunately, if q_u is small at any time along a re-entry trajectory, its exact value is unimportant. Under such circumstances either ablation is negligible, or the surface energy balance is dominated by radiation absorption.

3) When q_u is relatively small due to a large B_h, the heat and mass transfer correlations are particularly suspect. The correlations tend to be more accurate for the midrange of B_h values; the graphs presented by Gomez et al.,[3] suggest that it is not possible to obtain simple correlations which are accurate at large values of B_h.

4) For large ϕ and appreciable B_h, a comparison of the data in Tables 2 and 3 shows that whether choice of T_s or $\dot{m}_c$ for matching with the exact solution does have a significant effect on $\mathcal{R}$. Under these circumstances an inert injectant calculation cannot be precisely matched with an exact numerical solution, and $\mathcal{R}$ will not be a reliable indicator of the effect of gas-phase reactions.

With these sources of anomalous behavior accounted for, our preliminary assessment of the behavior of $\mathcal{R}$ as a function of ϕ, B_h, H_e, and p, is as follows:

An increase in ϕ is most simply viewed as an increase of the fraction of char products in the total ablation products. The surface temperatures associated with appreciable char removal are high and result in char products which do not further dissociate in the boundary layer. Thus, the char products should have little direct effect on $\mathcal{R}$. We cannot discern a significant trend in the data. In this context it is pertinent to note that the chemical domain of most significance to Apollo re-entry is located in the lower left hand quadrant of a graph with ordinate ϕ and percent coking as abscissa. Within the error limits imposed by the anomalous behavior just discussed, there is no discernible effect of B_h on $\mathcal{R}$.

Since T_s is nearly constant for the data presented, a decrease in H_e reduces the sensible enthalpy driving force available for conductive energy transport, and heat absorption or release due to gas-phase chemical reactions becomes relatively more significant; $\mathcal{R}$ shows a tendency to exceed unity as H_e decreases, thereby indicating that the dominant gas-phase reactions are indeed endothermic dissociations. Referring to the analysis of Cohen et al.,[22] we suggest that, under these circumstances, nonunity Lewis numbers strongly influence the behavior of $\mathcal{R}$.

The data for $\mathcal{R}$ at $p = 0.05$ and 0.10 atm are clearly too imprecise to yield useful information. However, the high wall enthalpies h_s at these pressures indicate a high degree of dissociation of the ablation products. Thus, the inert injectant calculation should be quite reliable in this situation. There is a definite tendency for $\mathcal{R}$ to exceed unity as p increases to 5 atm. This again confirms that the dominant gas-phase reactions are endothermic dissociations; at higher pressures the dissociations take place at higher temperatures and are therefore located further into the boundary layer.

Figure 3 shows concentration profiles for two situations: top) a relatively low T_s of 4537°R, where dissociation of H_2O and CO_2 occurs, and bottom) the more typical T_s of 6131°R, where the dominant ablation product reaction is dissociation of H_2.

Summary

1) The effect on surface heat transfer of gas phase chemical reactions involving ablation products can be isolated in the chemical energy recovery factor $\mathcal{R}$.

2) For Apollo re-entry conditions $\mathcal{R} \simeq 1$, hence surface heat transfer can be calculated accurately by assuming the species entering the boundary layer to be inert.

3) An engineering ablation prediction procedure has been developed; its essential element is the addition of an open-system, surface-equilibrium chemical state computation at selected time steps of a conventional finite-difference solution for the in-depth response of the ablator.

References

[1] Kendall, R. M., Bartlett, E. P., Rindal, R. A., and Moyer, C. B., "An Analysis of the Coupled Chemically Reacting Boundary Layer and Charring Ablator," CR 1060, 1968, NASA.

[2] Anfimov, N. A., "Heat and Mass Transfer Near the Stagnation Point with Injection and Suction of Various Gases Through the Body Surface," *Mekhanika Zhidkosti I Gaza*, Vol. 1, 1966, pp. 22–31.

[3] Gomez, A. V., Mills, A. F., and Curry, D. M., "Correlations of Heat and Mass Transfer for the Stagnation Region of a Re-entry Vehicle with Multicomponent Mass Addition," *Space Systems and Thermal Technology for the 70's Part II*, ASME, June 1970.

[4] Lees, L., "Convective Heat Transfer with Mass Addition and Chemical Reactions," *Third AGARD Colloquium on Combustion and Propulsion*, Pergamon Press, New York, 1959.

[5] Spalding, D. B., *Convective Mass Transfer*, McGraw-Hill, New York, 1963.

[6] Rosner, D. E., "Similtude Treatment of Hypersonic Stagnation Heat Transfer," *ARS Journal*, Vol. 29, 1959, pp. 215–216.

[7] Kendall, R. M., Rindal, R. A., and Bartlett, E. P., "Thermochemical Ablation," AIAA Paper 65-642, Monterey, Calif., 1965.

[8] Bartlett, E. P., Nicolet, W. E., and Howe, J. T., "Heat-Shield Ablation at Superorbital Re-entry Velocities," AIAA Paper 70-202, New York, 1970.

[9] Hirschfelder, J. O., Curtiss, C. F., and Bird, R. B., *Molecular Theory of Gases and Liquids*, 2nd ed., John Wiley, New York, 1964.

[10] Bird, R. B., "Diffusion in Multicomponent Gas Mixtures," *Kagaku Kogaku*, Vol. 26, 1962, pp. 718–721.

[11] Kendall, R. M., Rindal, R. A., and Bartlett, E. P., "A Multicomponent Boundary-Layer Chemically Coupled to an Ablating Surface," *AIAA Journal*, Vol. 5, No. 6, June 1967, pp. 1063–1071.

[12] Bartlett, E. P., Kendall, R. M., and Rindal, R. A., "A Unified Approximation for Mixture Transport Properties for Multicomponent Boundary-Layer Applications," CR 1063, 1968, NASA.

[13] Spalding, D. B., "A Standard Formulation of the Steady Convective Mass Transfer Problem," *International Journal of Heat and Mass Transfer*, Vol. 1, 1960, pp. 192–207.

[14] Svehla, R. A., "Estimated Viscosities and Thermal Conductivities of Gases at High Temperatures," TR R-132, 1962, NASA.

[15] Hochstim, A. R., "Equilibrium Compositions, Thermodynamics and Normal Shock Properties of Air with Additives," Vol. 1, Zph-122, 1961, General Dynamics-Convair.

[16] Wilke, C. R., "A Viscosity Equation for Gas Mixtures," *The Journal of Chemical Physics*, Vol. 18, 1950, pp. 517–519.

[17] Mason, E. A., and Saxena, S. C., "Approximate Formula for the Thermal Conductivity of Gas Mixtures," *The Physics of Fluids*, Vol. 1, 1958, pp. 361–369.

[18] Dergazarian, E. T. et al., *JANAF Thermochemical Tables*, Dec. 1960 and supplements to date, Thermal Lab., The Dow Chemical Co., Midland, Mich.

[19] Duff, R. E., and Bauer, S. H., "Equilibrium Composition of the C/H System at Elevated Temperatures," *The Journal of Chemical Physics*, Vol. 26, 1962, pp. 1754–1767.

[20] Kendall, R. M., and Bartlett, A. P., "Nonsimilar Solution of the Multicomponent Laminar Boundary Layer by an Integral-Matrix Method," *AIAA Journal*, Vol. 6, No. 6, June 1968, pp. 1089–1097.

[21] Kendall, R. M., "A General Approach to the Thermochemical Solution of Mixed Equilibrium-Nonequilibrium, Homogeneous or Heterogeneous Systems," CR 1064, 1968, NASA.

[22] Cohen, C. B., Bromberg, R., and Lipkis, R. P., "Boundary Layers with Chemical Reactions due to Mass Addition," *Jet Propulsion*, Vol. 28, 1958, pp. 659–668.